Desalination and Water Treatment
www.deswater.com
doi: 10.5004/dwt.2021.26925

220 (2021) 363–379
April

Mesoporous carbons as adsorbents to removal of methyl orange (anionic dye) and methylene blue (cationic dye) from aqueous solutions

Katarzyna Jedynak*, Marta Repelewicz, Krystyna Kurdziel, Dariusz Wideł

Institute of Chemistry, Jan Kochanowski University, Uniwersytecka 7, 25-406 Kielce, Poland, emails: kjedynak@ujk.edu.pl (K. Jedynak), martar@ujk.edu.pl (M. Repelewicz), krystyna.kurdziel@ujk.edu.pl (K. Kurdziel), dwidel@ujk.edu.pl (D. Wideł)

Received 7 October 2020; Accepted 11 December 2020

ABSTRACT

In this study, the removal of methyl orange (MO) and methylene blue (MB) from aqueous solutions using mesoporous carbon materials marked as ST-A and ST-A-CO_2 were investigated. The effects of different parameters that affect adsorption process such as contact time, pH, initial dye concentration, and temperature were studied. Removal of methyl orange from acidic solutions was more efficient than from basic solutions. In the case of methylene blue the reverse process was observed. To explain the kinetic model of adsorption, pseudo-first-order kinetic model, pseudo-second-order kinetic model, and the intraparticle diffusion model were used. The experimental data have been described by Langmuir, Langmuir–Freundlich, Freundlich, and Dubinin–Radushkevich adsorption isotherm models. The experimental data were fitted to the pseudo-second-kinetic model and Langmuir isotherm. Results of adsorption experiments showed that the studied carbons are characterized by high adsorption capacity in relation to the methyl orange and the methylene blue. The highest adsorption capacity was obtained for carbon ST-A-CO_2 (MO) (330 mg g^{-1} in temperature 315 K), lower successively for ST-A-CO_2 (MB) (222 mg g^{-1} in temperature 315 K), ST-A (MB) (187 mg g^{-1} in temperature 315 K), and ST-A (MO) (154 mg g^{-1} in temperature 315 K). Thermodynamic study showed that the adsorption was a spontaneous and endothermic processes ($\Delta G°$ ranges from –22.60 to –33.08 kJ mol^{-1} for all systems tested) and ($\Delta H°$ is 9.40, 8.12, 3.21, and 7.33 kJ mol^{-1} for ST-A (MO), ST-A-CO_2 (MO), ST-A (MB), and ST-A-CO_2 (MB), respectively).

Keywords: Adsorption; Methyl orange; Methylene blue; Mesoporous carbons; solution pH; Initial dyes concentration; Temperature; Isotherm; Kinetic; Thermodynamic

1. Introduction

The pollution of water is a global environmental problem which is connected with serious health problems, therefore many studies are conducted in order to find the permanent solutions of this problem [1].

Dyes, released from various industries and due to their extraordinary commonness are one of the group of hazardous substances that significantly pollute the aquatic environment [2–5]. Dyes are not only applied in the industry, for example, to the coloration of fabrics, but are added to food, to increase its attractiveness. Formerly most often natural dyes were applied. However, the rapid development of the industry caused the large growth of the use of synthetic dyes. This is particularly dangerous in case of the alimentary industry where studies showed their possible relationship with the cancer, allergies, and hypererethism, particularly in case of children [6].

Methyl orange (MO) is an azo dye, classified as an anionic dye. Azo dyes are the greatest (above 50% all dyes) and most important class of synthetic organic dyes due to their light colors, the durability, the easy application, the chemical stability, and the versatility [7]. MO has been applied in the paper manufacturing, textile, printing, pharmaceutical, food, biomedical, chemical, and technological

* Corresponding author.

1944-3994/1944-3986 © 2021 Desalination Publications. All rights reserved.

industries and in research laboratories [8–10]. Methyl orange, as many other dyes from this class, is carcinogenic and toxic. Its action relies on the random absorption to the organism where it is metabolized to the aromatic amine through intestinal microorganisms. Reducing enzymes, present in the liver, can catalyze the reductive breaking of the azo bond to aromatic amines what may cause intestines cancer. Still, the toxicity of this dye is not determined quantitatively, but it is proved that high concentration in living organisms could be harmful [10].

Methylene blue (MB) is one of the most commonly cationic, thiazine dyes. MB is used for dying cotton, wood, leather, and silk, also for medical and antiseptic purposes and in chemistry, biology, and in the laboratories [11–14]. This dye can cause permanent injury to the eyes and skin and induce some negative effects on living beings such as: delirium, excessive sweating if inhaled through water, diarrhea, vomiting, irritation of mouth, throat, and stomach with symptoms of nausea [15].

Organic dyes present in the wastewater endangers not only to the environment (water and soil) but also to human life (even at low concentration) [16,17]. Due to the fact that they have a complex molecular structure (as an aromatic compounds they contain different groups, like phenyl, amino, and azo) and synthetic origin, they are highly toxic, carcinogenic in nature, chemically stable, and difficult for biodegradation [1,2–5,15]. These dyes are increasingly applied because of their easiness of use, low cost of synthesis, and variety of color compared with natural dyes [1].

Therefore, it is of great importance to develop the effective treatment techniques for the removal of dyes from environment [18]. For this purpose, various processes are used, such as photocatalytic degradation, coagulation, ozonation, ion exchange, reverse osmosis, and adsorption [1,16]. The adsorption process among all techniques of dyes removal from water is considered as the most effective and efficient due to its low cost and flexibility in design [19–22]. Over the recent years of the adsorption became a most powerful tool of purification and separation. This process is controlled by different parameters such as: the temperature, the time of the contact, the initial concentration of the adsorbate, the dose of the adsorbent, the pH, the particles size of the adsorbent, etc., and this process takes place in the most natural, chemical, biological and physical systems [1]. The equipment used in this process is uncomplicated and easy to operate [7]. Therefore, the most important element is to find appropriate adsorbents that can adsorb dyes from the water environment in the shortest possible time and with the greatest efficiency [8,9]. In recent years, many studies have been carried out on the adsorption of dyes on various solid adsorbents (very often on carbon adsorbents), used widely for purification of wastewater, water, and in industrial applications.

The adsorbents used to remove methyl orange from the aquatic environment are commercial carbons [23,24], laboratory carbons obtained from various polymer precursors [23,24], activated carbons including activated carbons with silicon carbide nanoparticles [25], from common reed (*Phragmites australis*) [26] and Jerusalem artichoke stalk [27], multiwalled carbon nanotubes [28], hexagonal-shaped carbon materials [29], and waste materials [10].

The adsorbents used in the methylene blue adsorption process are: biochar [30–36], Fe–Mn binary oxide nanoparticles [5], activated carbon [14,37–42], carbon nanotubes [43], waste produced [44,45], natural zeolites [46], and metal organic framework (MOF) [15,47].

The most popular in the adsorption process are mesoporous carbons [26,48,49], mesoporous TiO_2 [50], and also modified mesoporous carbons [2,51–56] due to their unusual properties such as large surface area, ordered pore structure, large pore volume, narrow pore size distribution, and the possibility of modifying the pore diameter.

The aim of this work was to determine the possibility of the use of two, earlier synthesized by soft-templating method, mesoporous carbons (STA and STACO_2) [57] to the removal of the methyl orange and the methylene blue from aqueous solution. The way of the synthesis and the physicochemical characteristics of these carbon adsorbents were presented in our earlier publication [57].

The investigations were undertaken to determine the factors influencing on the process of the adsorption, of mentioned dyes, such as: the time of the contact, the pH of the solution, the initial concentration of the dye, and the temperature. For the interpretation of obtained experimental isotherms of the adsorption following two-parameters models were applied: Langmuir, Freundlich, Langmuir–Freundlich, and Dubinin–Radushkevich. To describe the rate of the adsorption equilibrium state achievement in examined systems, three selected kinetic models were applied: pseudo-first-the order, pseudo-secondo-order, and intraparticle diffusion the model.

Determined constants of the adsorption rate and constants of equilibrium of this process will give the possibility of the thermodynamic ($\Delta G°$, $\Delta H°$, and $\Delta S°$) parameters calculations which will allow the full description of nature of examined processes. Based on the experimental results, the interaction mechanism in the adsorption processes between the dyes and the tested carbons was proposed.

2. Materials and methods

2.1. Adsorbates and adsorbents

Methyl orange (85% of purity) and methylene blue (96% of purity) were supplied by Sigma-Aldrich (Germany). The chemical structures of the two dyes are presented in Fig. 1.

The two synthesized mesoporous carbons were marked as ST-A and ST-A-CO_2. Mesoporous carbon (ST-A) was prepared by the soft-templating method according to a slightly modified recipe presented in work [58] and like that reported in the work [59]. Adsorbent ST-A-CO_2 was obtained of ST-A carbon by its activation with CO_2, according to a slightly modified recipe of [60]. The detailed synthesis description was presented in our previous article [57].

2.2. Adsorption experiments

Adsorption studies were carried out in 100 mL Erlenmeyer's flasks in incubator (Orbital Shaker – Incubator ES-20, Grant-bio) for defined time. Volume of 50 cm^3 of previously prepared solutions of MO or MB, with various concentrations (Table 1), were added into conical flasks with 0.1 g of examined carbons, then shaken in the incubator at 200 rpm.

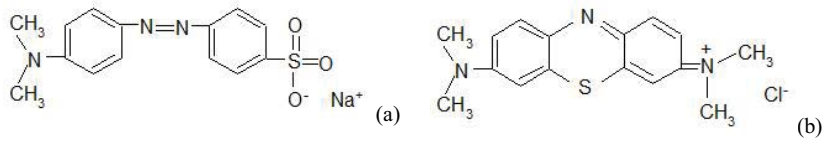

Fig. 1. Chemical structures of MO (a) and MB (b).

Concentrations of dyes before and after the adsorption process were determined by the spectrophotometrical method (SP-830 the Plus from Metertech) conducting the measurement of the absorbance in the maximum of the absorption at 465 nm for MO and 665 nm for MB. Applied wavelengths were determined on the basis of absorption spectra of studied dyes. Detailed data concerning the conditions of the adsorption processes are presented in Table 1.

The influence of pH on adsorption process was examined. For that purpose, the solutions of studied dyes were prepared in the pH range from 2 to 10 by adding HCl (0.1 or 1.0 mol dm^{-3}) or NaOH (0.1 or 1.0 mol dm^{-3}). Investigations were conducted by pH-meter, model inoLab pH 730 from WTW. Detailed data concerning the conditions of the measurement are presented in Table 1.

3. Results and discussion

3.1. Characterization of studied carbons

Detailed characterization of the studied adsorbents is presented in the work [57]. Investigated carbons have large surface area: ST-A: 710 $m^2 g^{-1}$ and ST-A-CO_2: 950 $m^2 g^{-1}$, and developed porosity, V_t is: 0.71 and 0.81 $cm^3 g^{-1}$, respectively. It must be mentioned that in both studied carbon materials mesopores volume dominates. Carbon material activated by CO_2 has a bit more developed microporosity. Both studied carbons have acidic properties (total basic groups for ST-A: 0.30 mmol g^{-1} and for ST-A-CO_2: 0.56 mmol g^{-1}, total acidic groups: 0.72 and 0.82 mmol g^{-1}, respectively). There are phenolic and carbonyl groups on the surface of investigated adsorbents. The values of pH_{PZC} for ST-A and ST-A-CO_2 are 8.06 and 7.73, respectively.

3.2. Adsorption properties

3.2.1. Effect of the solution pH

The pH of the solution is a very important issue in the adsorption process of the dyes on carbon adsorbents, from aqueous solutions.

The first studied in this work dye, which is methyl orange, can be present in the solution basically in two different forms: alkaline (deprotonated – azo, form I) and acidic (protonated – quinonoid, form II) [4,8]. First of these two forms can be present in solutions with higher pH value, second form in acidic solutions. In Fig. 2 two forms of MO are shown, in order to pH value of the solution.

The second of investigated in this work dyes, methylene blue, is present in the aqueous solutions also in two forms [61]. In alkaline environment, it is present as a form with one positive charge localized on sulfur atom (form I) and in acidic environment hydrogen ions are attached to the nitrogen atom of one of the dimethylammonium group, creating final form with two positive charges (form II). Forms of MB in order to solution pH are presented in Fig. 3.

The efficiencies of dyes removal from solutions in the pH range of 2–10 on the tested adsorbents are presented in Fig. 4. Applied in this work pH range was based on MO works [2,48] and MB work [62].

As it can be seen in Fig. 4 adsorption of both dyes is depended on pH value. Adsorption of MO (Fig. 4a) decreases initially with the increase of pH value, but from pH = 4 stabilize at constant level. At pH = 2, the % removal of MO is for ST-A: 88% and for ST-A-CO_2: 99%. Similar dependence was observed in works [2,48] for MO adsorption on carbon adsorbents. In the case of higher pH, values reaches: for ST-A: approximately 60% and for ST-A-CO_2 approximately 90%. In the case of MB the opposite effect can be observed (Fig. 4b). There is an increase of the adsorption for higher pH values of the solution. The % removal is for ST-A: 88% and for ST-A-CO_2: 99%, at pH 8–10. In work [63] the similar influence of solution pH on adsorption process of MB on carbon adsorbent was observed. Differential sorption capacity of investigated systems can be explained taking into consideration the charge accumulated on the surface of studied carbons and the forms of dyes. According to the literature [64,65] for pH > pH_{PZC} the surface charge is negative, while pH < pH_{PZC} the surface is positively charged. The determined values of pH_{PZC} for studied carbons are:

Table 1
Adsorption conditions studies

Experimental item	Adsorbent	MO solution concentration (mg dm^{-3})/sampling time (h)	MB solution concentration (mg dm^{-3})/sampling time (h)	Temperature (K)
Adsorption isotherms	ST-A	100–1,000 or 1,400/8 h	70–1,100/4 h	298,308,315
	ST-A-CO_2	400–1,800/8 or 6 h	100–800/3 or 2 h	298,308,315
Adsorption kinetics	ST-A	100/0.5–24 h	100/0.25–6 h	298,308,315
	ST-A-CO_2	400/0.5–24 h	100/0.25–4 h	298,308,315
Solution pH	ST-A	200/4 h	200/4 h	298
	ST-A-CO_2	400/4 h	400/4 h	298

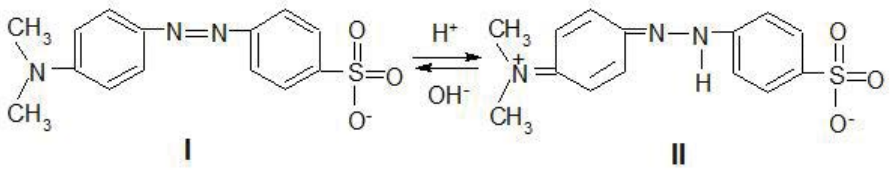

Fig. 2. Two forms of the MO in order to solution pH.

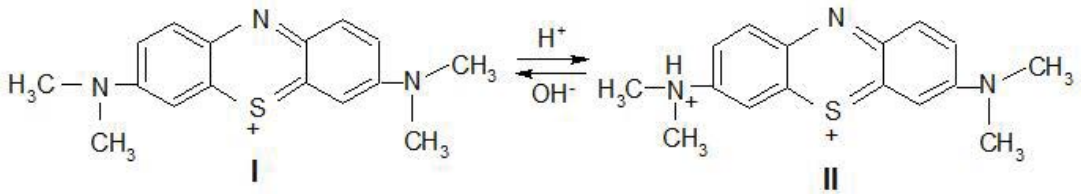

Fig. 3. Two forms of the MB in order to solution pH.

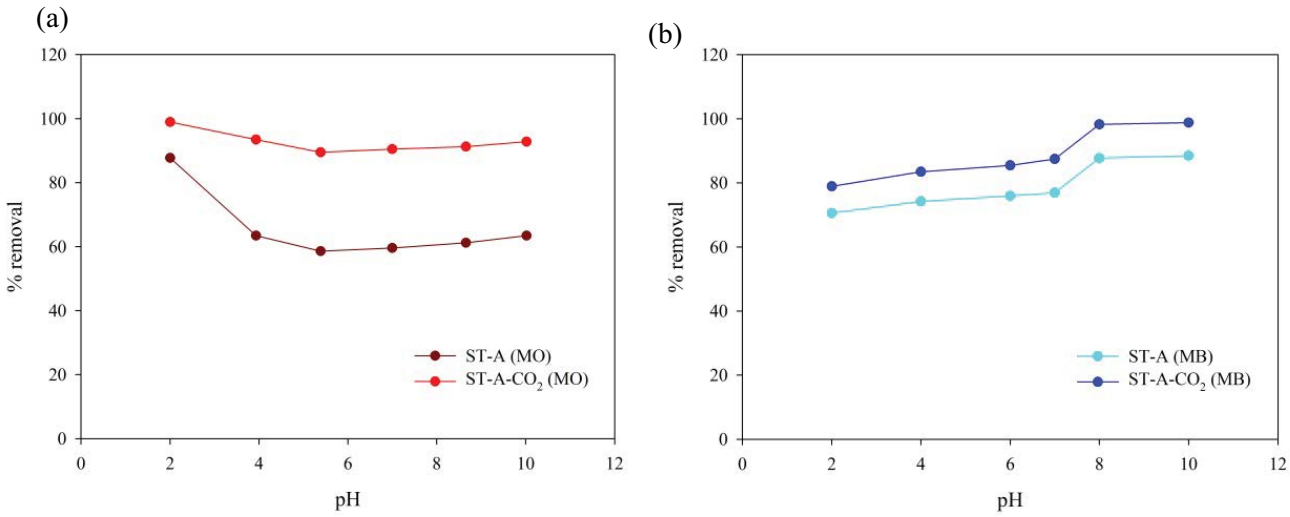

Fig. 4. Effect of the pH on the MO (a) and MB (b) adsorption process for studied adsorbents.

ST-A: 8.06; ST-A-CO_2: 7.73. Considering electrostatic interactions adsorbent-adsorbate, anionic MO is stronger adsorbed on the positively charged surface of the adsorbent (pH < pH_{PZC}), for the pH value lower than pH_{PZC}. The MB, as a cationic dye, is adsorbed stronger on the negatively charged surface of the carbon.

3.2.2. Adsorption kinetics

3.2.2.1. Effect of contact time

The dependence of adsorption vs. time of the process for MO and MB on investigated adsorbents in three temperatures (298, 308, and 315 K) is presented in Figs. 5a–d. In the case of studied systems, the adsorption initially increases rapidly, then the kinetic equilibrium is being set. The adsorption rate of MO (Fig. 5a and b) on both studied adsorbents in investigated temperatures were set at a constant level after 8 h, except ST-A-CO_2. On this adsorbent, in temperature 315 K, the equilibrium was set much earlier, after 6 h (Table 1). Adsorption of MB (Figs. 5c and d) on both adsorbents was much faster, because after 4 h. Like in the case of MO for ST-A-CO_2 in temp. 315 K, the constant state was achieved just after 2 h (Table 1).

3.2.2.2. Kinetics models

In this study, three kinetic models, namely pseudo-first-order model, known also as Lagergren Eq. (1) [66] and pseudo-second-order model called the Ho Eq. (2) [67] and Weber–Morris intraparticle diffusion model Eq. (3) [68] were used to describe the MO and MB adsorption kinetics from aqueous solutions on the studied carbon materials:

$$\ln\left(q_e - q_t\right) = \ln q_e - k_1 t \tag{1}$$

$$\frac{t}{q_t} = \frac{1}{k_2 q_e^2} + \frac{t}{q_e} \tag{2}$$

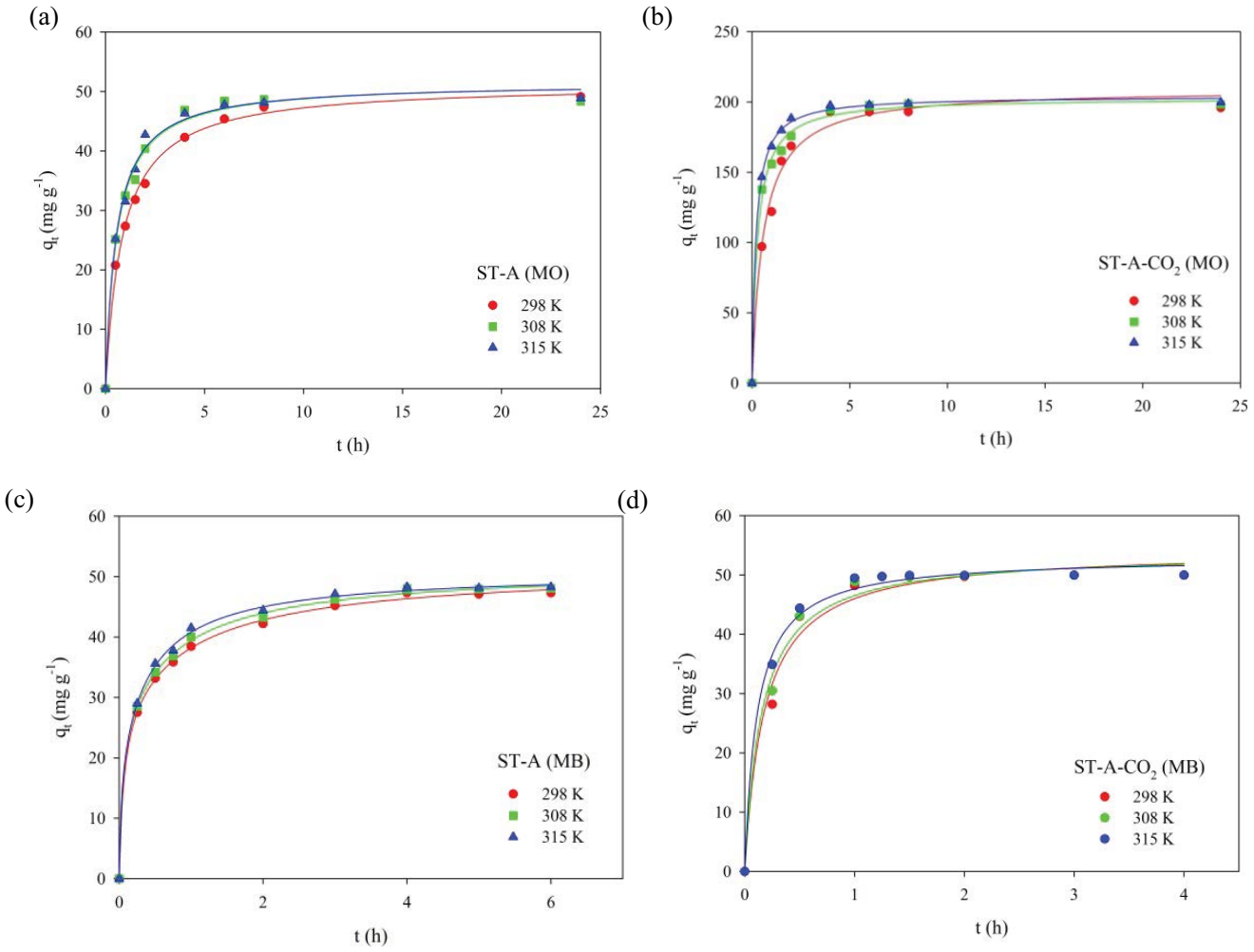

Fig. 5. Experimental kinetic data (a–d) of MO and MB on studied carbon materials (ST-A, ST-A-CO_2, respectively).

$$q_t = k_{id} t^{1/2} + c \quad (3)$$

where k_1 is the pseudo-first-order rate constant (h^{-1}); k_2 is the pseudo-second-order rate constant (g mg^{-1} h^{-1}); t is the time of contact between the adsorbent and adsorbate (h); q_e is the adsorption value after the equilibrium stabilization (mg g^{-1}); q_t is the adsorption value in given time t (mg g^{-1}), respectively; k_{id} is the intraparticle diffusion rate constant (mg g^{-1} h$^{-1/2}$); and c is the intercept, which represents the thickness of the boundary layer (mg g^{-1}).

The linear relationships resulting from the presented pseudo-first-order (Eq. (1)) and pseudo-second-order kinetic models (Eq. (2)) for the adsorption of MO and MB on the studied adsorbents are showed in Figs. 6a–d and 7a–d. The kinetic parameters and correlation coefficients were presented in Table 2. Based on obtained results and considering the value of R^2 coefficient higher than 0.98 it is hard to decide which model describes the rate of adsorption process. However, considering the general dependence, that the reaction rate constant increases with temperature rise, obtained results suggest that it is pseudo-second-order reaction. The values of rate constants k_2 for both studied adsorbents and adsorbates increase evenly with increasing temperature in investigated systems. This dependence is not preserved for rate constant k_1. In the case of studied dyes the kinetics of adsorption process on the other carbon materials is described most often by pseudo-second-order model and for example for MO [4,19,24–28,48,52,54,55] and for MB [30,31,38,39,43].

In Figs. 8a–d the amount of adsorbed adsorbate vs. $t^{1/2}$ is shown, for both studied materials. For ST-A carbon, in case of both adsorbates, on diagrams (Figs. 8a and c) three linear sections can be noticed. While for ST-A-CO_2 on diagrams (Figs. 8b and d) there are two linear sections. Obtained diagrams can be an explanation to the intraparticle diffusion influence on the rate of adsorption process. The interpretation of the influence of the adsorption process rate based on the Weber–Morris equation is relatively difficult. There are two possible approaches to this issue in the literature [34,63,69]. The first one assumes that there is a linear dependence between q_t and $t^{1/2}$ (among whole range of investigated time to the equilibrium state), which can traverse or not the origin of the coordinate system. When the plot passes through the origin of the coordinate system it can be assumed, that the intraparticle diffusion

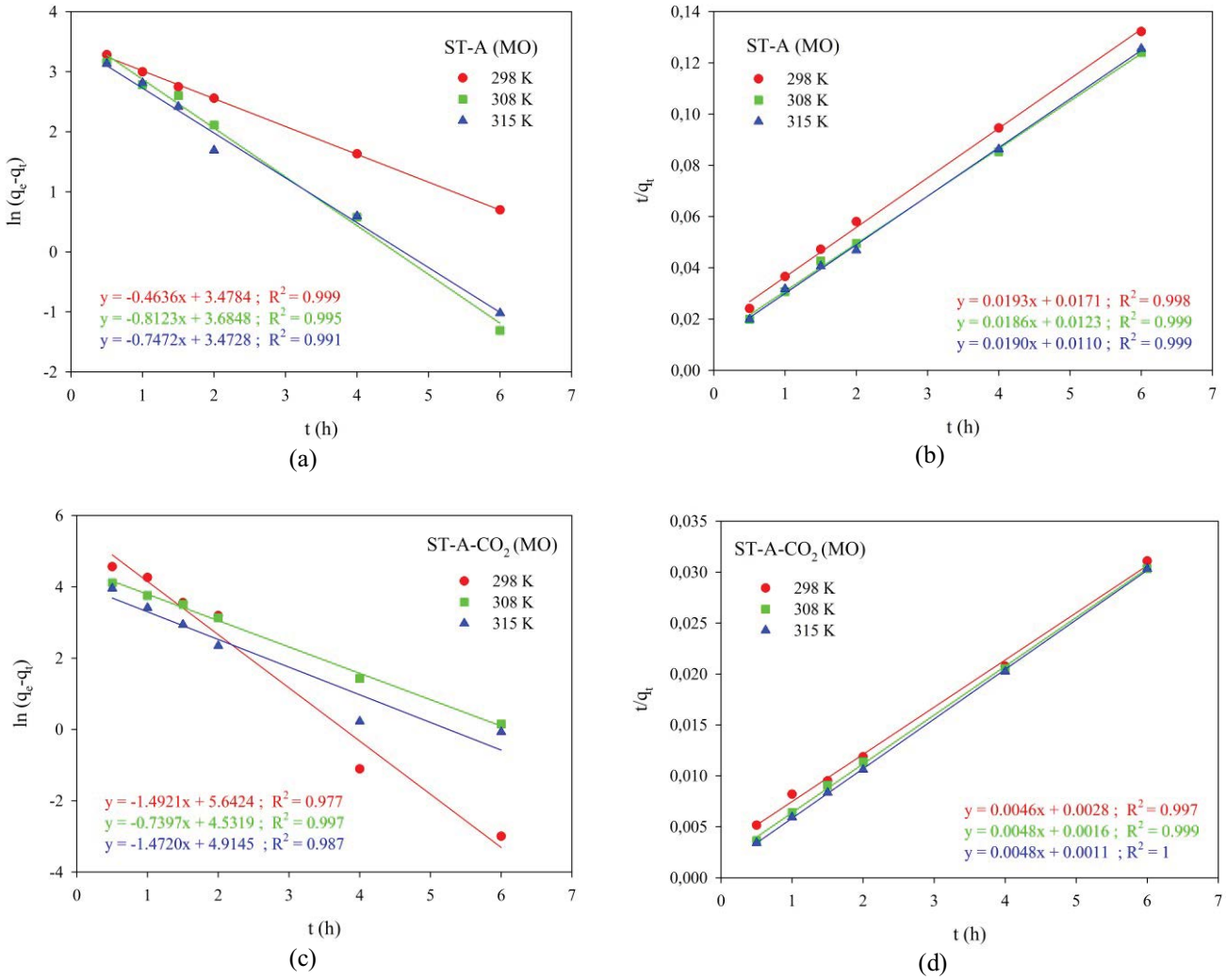

Fig. 6. Pseudo-first-order (a and c) and pseudo-second-order model (b and d) for ST-A (MO), ST-A-CO_2 (MO).

Table 2
Kinetics parameters for the adsorption of MO and MB on examined adsorbents

Adsorbate	Adsorbent	Temperature (K)	Pseudo-first-order		Pseudo-second-order	
			k_1 (h^{-1})	R^2	k_2 (g mg^{-1} h^{-1})	R^2
MO	ST-A	298	0.4636	0.999	0.0218	0.998
		308	0.8123	0.995	0.0281	0.999
		315	0.7472	0.991	0.0328	0.999
	ST-A-CO_2	298	1.4921	0.977	0.0075	0.997
		308	0.7397	0.997	0.0144	0.999
		315	1.4720	0.989	0.0209	1
MB	ST-A	298	0.7624	0.988	0.0901	0.999
		308	0.8077	0.983	0.0925	0.999
		315	0.9548	0.981	0.0952	0.999
	ST-A-CO_2	298	3.557	0.997	0.0851	0.993
		308	3.597	0.997	0.0911	0.997
		315	4.363	0.995	0.1296	0.999

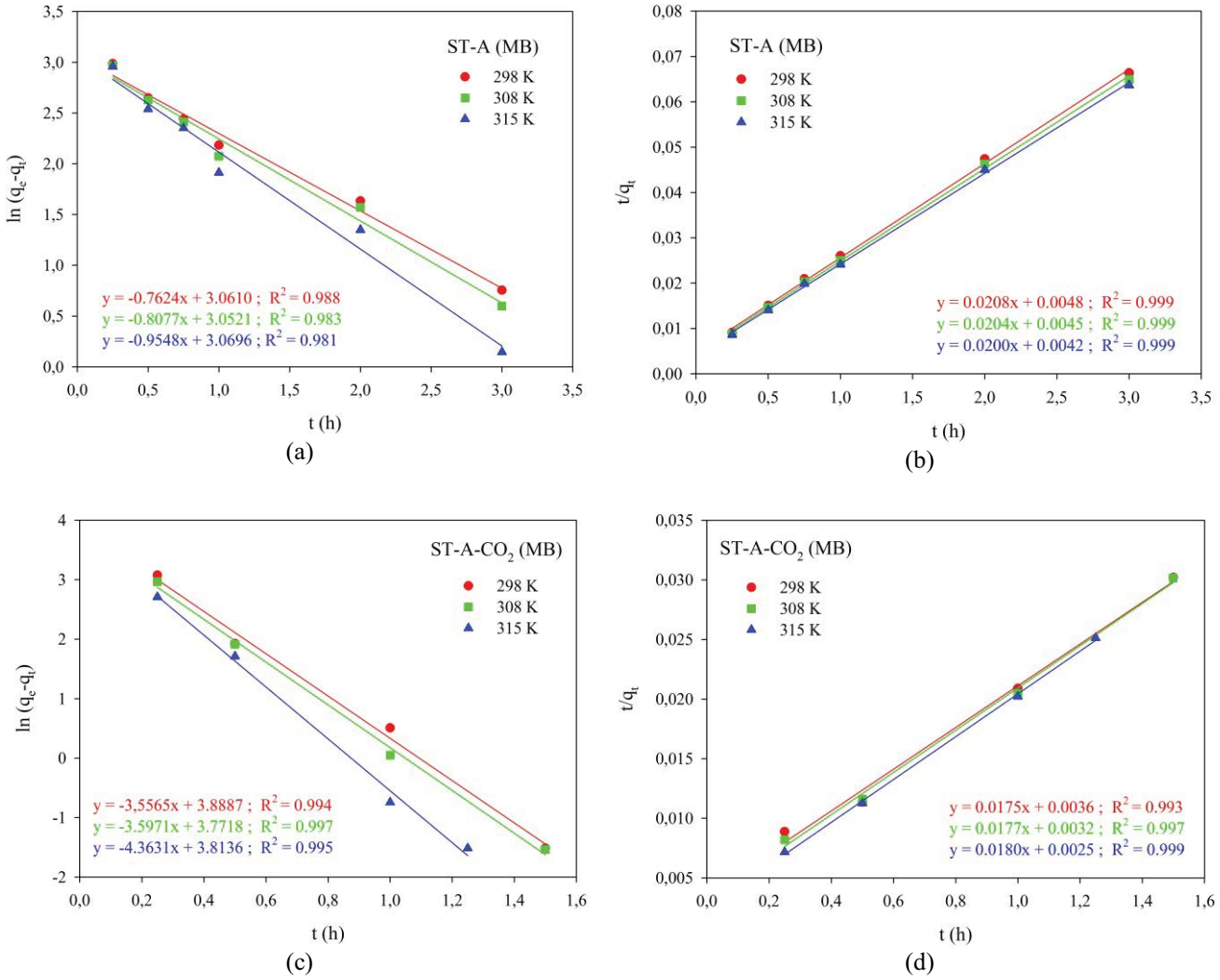

Fig. 7. Pseudo-first-order (a and c) and pseudo-second-order model (b and d) for ST-A (MB), ST-A-CO_2 (MB).

is a stage that limits the rate of whole adsorption process. If the plot does not pass, the intersection point with the ordinate corresponds to the thickness of the boundary layer. The second approach considers the multilinearity of the dependence q_e vs. $t^{1/2}$, which can be composed with two or three straight lines. Multilinearity can be observed in the case when other processes can influence the rate of the adsorption, not only the intraparticle diffusion.

The results obtained in this work can be interpreted according to second approach. For ST-A systems in MO and MB solutions, three straight lines were obtained. First two response for the intraparticle diffusion and the third one describes the adsorption equilibrium state. For first two straight lines values of constants k_{id1} and k_{id2} were calculated (Table 3). The values of k_{id1} for both dyes are similar in three investigated temperatures, while the temperature increase the k_{id2} value changes distinctly. For ST-A (MO) k_{id1} values decrease from 10.67 to 4.95 mg g^{-1} $min^{-1/2}$ and for ST-A (MB) the values change from 9.21 to 7.64 mg g^{-1} $min^{-1/2}$. The first section of the plot can be interpreted as a diffusion in large pores, while second as a diffusion in pores of small dimensions (meso–micropores). For the ST-A-CO_2 systems, in presence of both studied adsorbates, two straight lines were obtained. First one relates to intraparticle diffusion and second one corresponds to equilibrium achievement. Calculated values of k_{id1} from Eq. (3) (Table 3) distinctly decrease with the temperature and what is characteristic they are much higher than in case of ST-A adsorbent (Table 3). For example, for ST-A CO_2 in 298 K temperature, k_{id} is 107.07 mg g^{-1} $min^{-1/2}$ and for the same adsorbate for ST-A carbon in the same temperature k_{id} value is 10.67 mg g^{-1} $min^{-1/2}$. It should be noticed that the adsorption equilibrium on ST-A-CO_2 carbon (Table 3) was reached faster than on ST-A carbon, what can be a result of significant differences of diffusion rate constants values. Calculated values of "c" parameter from Eq. (3) (Table 3) for studied in this work systems, aren't equal to zero and have positive values, which suggests that intraparticle diffusion isn't the stage that limits the course of adsorption process.

Summarizing, in both cases we can talk about the influence of the intraparticle diffusion on the rate of adsorption process, but it isn't the limiting stage.

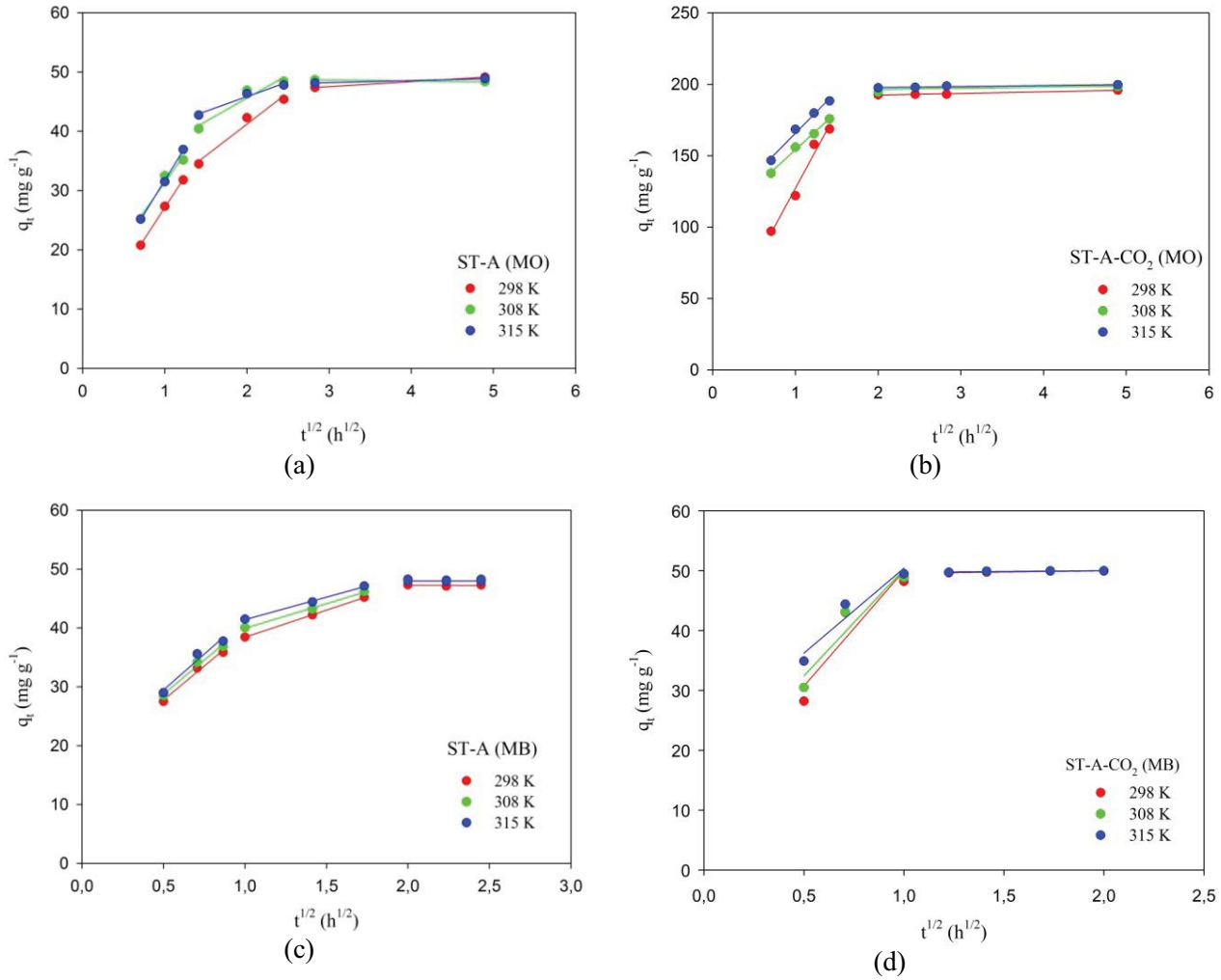

Fig. 8. Intraparticle diffusion (a and b) (MO), (c and d) (MB) for ST-A, ST-A-CO_2, respectively.

Table 3
Intraparticle diffusion model parameters

Adsorbent (Adsorbate)	Temperature (K)	k_{id1} (mg g^{-1} h$^{-1/2}$)	c_1 (mg g^{-1})	R^2	k_{id2} (mg g^{-1} h$^{-1/2}$)	c_2 (mg g^{-1})	R^2
	298	21.37	5.75	0.999	10.67	19.88	0.972
ST-A (MO)	308	19.72	11.66	0.966	7.87	29.86	0.930
	315	22.64	9.07	0.999	4.95	35.95	0.973
	298	23.01	16.28	0.984	9.21	29.22	1
ST-A (MB)	308	23.01	17.28	0.984	8.36	31.60	0.996
	315	24.36	17.29	0.957	7.64	33.79	0.997
	298	107.07	20.06	0.975	–	–	–
ST-A-CO_2 (MO)	308	52.94	101.19	0.994	–	–	–
	315	58.86	106.89	0.985	–	–	–
	298	38.58	11.41	0.870	–	–	–
ST-A-CO_2 (MB)	308	35.66	14.58	0.906	–	–	–
	315	28.36	22.06	0.928	–	–	–

3.2.3. Adsorption isotherms

In Fig. 9 experimental adsorption isotherms of MO and MB on ST-A and ST-A-CO_2, obtained in 298 K are shown.

When analyzing the presented graphs for both tested dyes, we observe that ST-A-CO_2 carbon is a much better adsorbent, in comparison to ST-A. For ST-A-CO_2 maximum adsorption is 323 mg g^{-1} (MO) and 192 mg g^{-1} (MB). Much lower values of the adsorption capacity for ST-A (117 mg g^{-1} (MO) and 135 mg g^{-1} (MB)) were obtained.

Four equilibrium isotherm models, namely the Langmuir [70], the Freundlich [71], the Langmuir–Freundlich [3], and the Dubinin–Radushkevich [62,72,73] were used to fit the experimental data. The Langmuir (Eq. (4)), the Freundlich (Eq. (5)), the Langmuir–Freundlich (Eq. (6)), and the Dubinin–Radushkevich (Eq. (7)) isotherm models were presented in Eqs. (4)–(7), respectively.

$$q_e = \frac{q_m K_L C_e}{1 + K_L C_e} \tag{4}$$

$$q_e = K_F C_e^{1/n} \tag{5}$$

$$q_m = \frac{q_m \left(K_{LF} C_e\right)^m}{1 + \left(K_{LF} C_e\right)^m} \tag{6}$$

$$q_e = q_m e^{-\beta\varepsilon^2} \tag{7}$$

where q_m is the maximum adsorption capacity corresponding to the total monolayer coverage on the adsorbent surface (mg g^{-1}); K_L is the Langmuir constant (dm^3 g^{-1}), K_F is the Freundlich isotherm constant ($mg^{(1-1/n)}$ $(dm^3)^{1/n}$ g^{-1}); n is empirical constant describing the heterogeneity of the adsorbent surface, K_{LF} is the Langmuir–Freundlich constant (dm^3 mg^{-1}); m is constant, ε is Polanyi potential (Eq. (8)); β is connected with adsorption energy (E) (Eq. (9)), which is defined as the free energy transfer of 1 mol of solute from infinity of the surface of the sorbent.

Polanyi potential (ε) and adsorption energy (E) were calculated on the basis of equations:

$$\varepsilon = RT \ln\left(1 + \frac{1}{C_e}\right) \tag{8}$$

$$E = \frac{1}{\sqrt{2\beta}} \tag{9}$$

The non-linear regression model using Origin Microcal 10 (together with the Levenberg–Marquardt algorithm) was applied in order to attribute an appropriate adsorption model and calculate adsorption parameters characteristic for each model.

Experimental values of the MO and MB adsorption on studied carbon materials in function of equilibrium concentration of dye solution complied with curves determined on the basis of four selected models (Langmuir, Freundlich, Langmuir–Freundlich, and Dubinin–Radushkevich) were presented on Figs. 10 and 11. Based on the graphic image of the discussed diagrams it is very difficult to choose the appropriate model of the adsorption. The solution to this problem is provided by the calculated parameters characterizing adsorption process described according to selected theoretical equations (Table 4). It results, from the data shown in Table 4, that the appropriate model describing the adsorption process of both studied dyes on all investigated carbon adsorbents is the Langmuir isotherm. This is evidenced by the maximum adsorption capacity values (q_m), similar to experimental values ($q_{m,exp}$), and also regular (in order to increasing temperature) change of the equilibrium constants K_L and high values of the correlation coefficients R^2. In the case of studied in this work dyes, adsorption process on carbon adsorbents is described most often by Langmuir equation, for example for MO in works [2,25,27,53] and for MB in works [30–32,38,39,43].

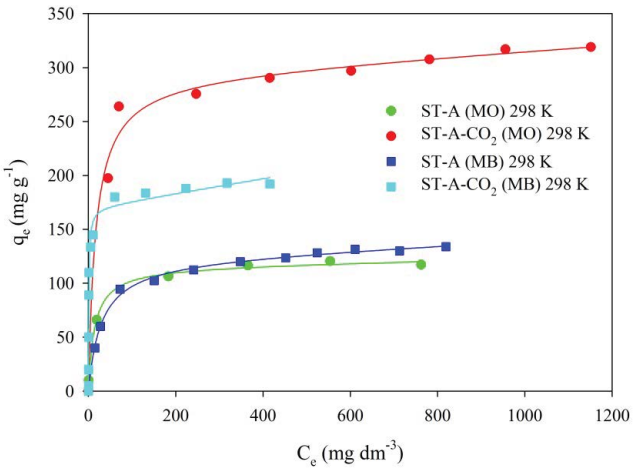

Fig. 9. Experimental adsorption isotherms of MO and MB on tested carbon materials in temperature 298 K.

The parameters determined using the Langmuir, Langmuir–Freundlich, Freundlich, and Dubinin–Radushkevich adsorption isotherm models are presented in Table 4.

The MO and MB adsorption on studied carbons vs. temperature of the process is presented in Figs. 12a–d. For both studied carbon materials, with temperature rise, adsorption increase, which proves the endothermic character of the discussed process. In the case of MO adsorption for ST-A is changing from 117 mg g^{-1} in 298 K temperature to 154 mg g^{-1} in 315 K temperature, and for ST-A-CO_2 is changing from 323 mg g^{-1} in 298 K temperature to 330 mg g^{-1} in 315 K temperature. For MB adsorption, the situation is analogous (ST-A: from 135 mg g^{-1} in 298 K temperature to 187 mg g^{-1} in 315 K temperature; ST-A-CO_2: from 192 mg g^{-1} in 298 K temperature to 222 mg g^{-1} in 315 K temperature).

3.3. Adsorption thermodynamics and isosteric heat of adsorption

To completely understand the adsorption nature the following functions were designated, describing the thermodynamics of studied adsorption processes: free enthalpy (ΔG°), enthalpy (ΔH°), and entropy (ΔS°) [62].

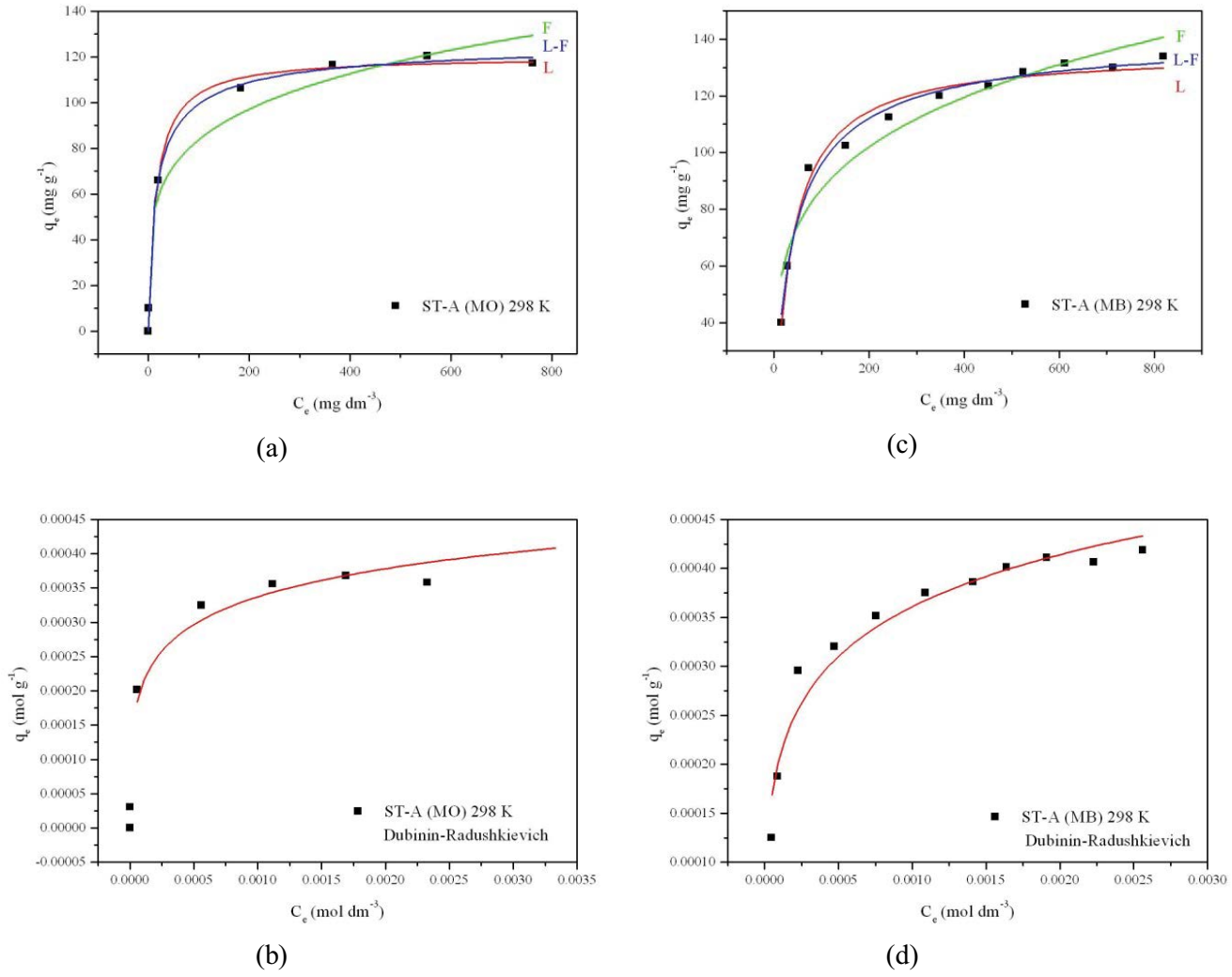

Fig. 10. Langmuir, Langmuir–Freundlich, Freundlich, and Dubinin–Radushkevich isotherms in temperature 298 K for ST-A (a and b) MO, (c and d) MB.

$$\Delta G^\circ = -RT\ln K_L \tag{10}$$

$$\ln K_L = -\frac{\Delta H^\circ}{R}\times\frac{1}{T}+\frac{\Delta S^\circ}{R} \tag{11}$$

The dependence $\ln K_L = f(1/T)$ for all investigated adsorbents are presented in Fig. 13. The calculated values of ΔG°, ΔH°, and ΔS° are listed in Table 5.

The negative values of ΔG° in all the studied temperatures indicate that the adsorption processes of dyes studied on the mesoporous carbons is spontaneous in nature. The positive values of ΔH° implies the endothermic character of the adsorption process in all studied systems. The positive values of ΔS° mean that the randomness at the solid/solution interface increased during adsorption.

The isosteric heat of adsorption (ΔH_x) can be determined on the basis of the dependence $\ln C_e = f(1/T)$ for the given values of the coverage degree of the surface. This dependence is a consequence of Clausius–Clapeyron. The value of ΔH_x calculated from the Clausius–Clapeyron equation [62,74]:

$$\left(\frac{d\ln C_e}{dT}\right)_{q_e} = -\frac{\Delta H_x}{RT^2} \tag{12}$$

The linear relationship is presented in the following equation:

$$\ln C_e = \frac{\Delta H_x}{R}\times\frac{1}{T}+\text{const} \tag{13}$$

The obtained values of isosteric heat of adsorption (ΔH_x) calculated from the Eq. (13) are presented in the Table 6.

For ST-A (MB) and ST-A-CO_2 (MB) the isosteric heat of adsorption increases with the increase of surface coverage. For MO, no such relationship is observed.

Table 7 compares the maximum adsorptive capacity (q_m) of studied in this work carbon materials with other adsorbents used in literature for removal of MO and MB. Our carbons are characterized by better properties in comparison to other adsorbents.

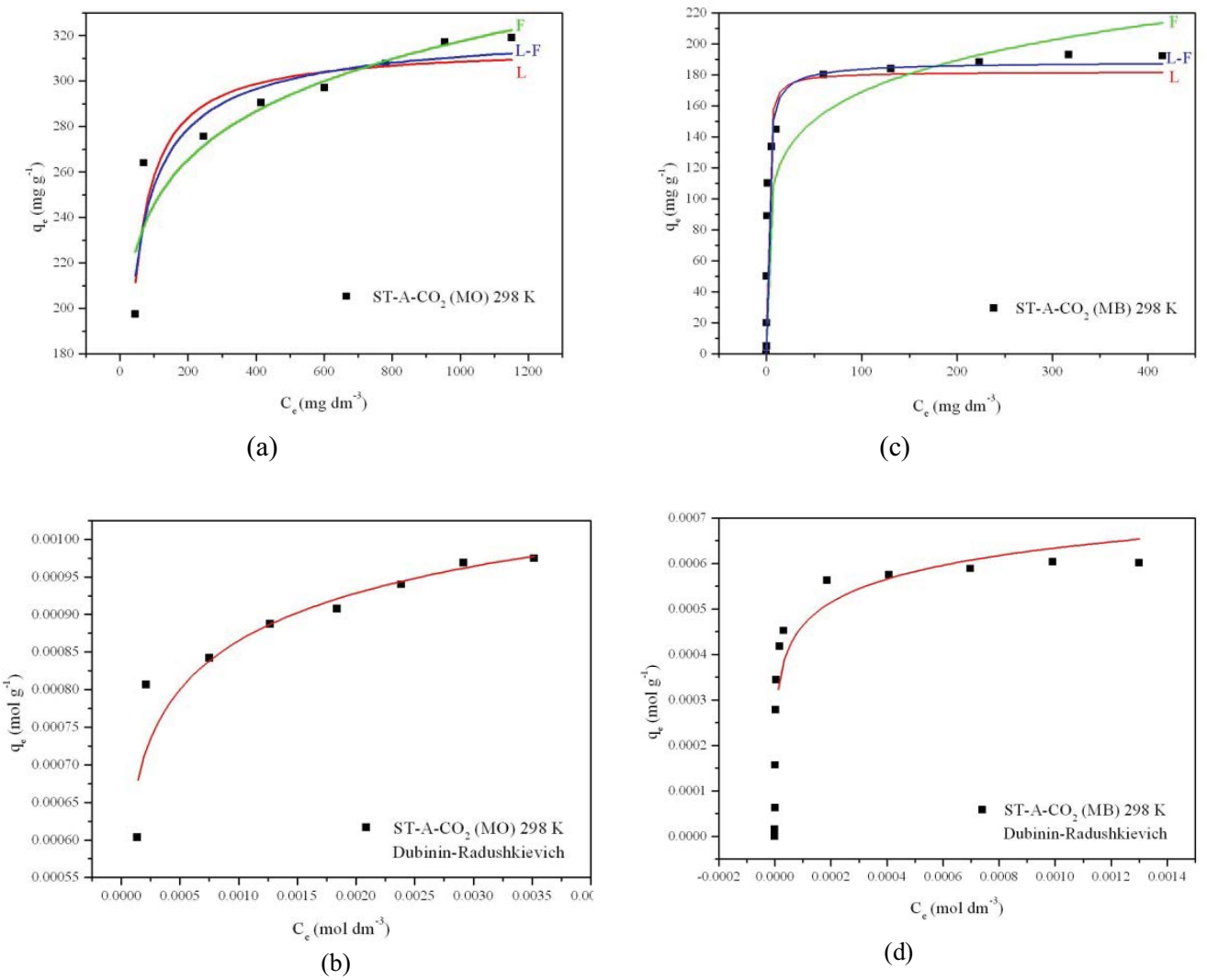

Fig. 11. Langmuir, Langmuir–Freundlich, Freundlich, and Dubinin–Radushkevich isotherms in temperature 298 K for ST-A-CO_2 (a and b) MO, (c and d) MB.

4. Conclusions

In this work, it has been shown that the tested carbon materials (ST-A and ST-A-CO_2) are promising adsorbents for methyl orange and methylene blue.

Investigations on influence of various parameters such as contact time, pH, initial dye concentration, and temperature on removal of MO and MB have been carried out.

It was showed that the adsorption of MO and MB on both examined investigated carbons coals depended on the pH of solution in the different way. In case of MO initially it decreases but from the pH = 4 it stabilizes on the constant level at approximately 60% for ST-A and 90% for ST-A-CO_2 carbon. However, in case of MB the growth of the pH favours the adsorption. In basic solutions (pH = 8–10) the efficiency of the removal process of this dye is very high at 88% for ST-A and 99% for ST-A-CO_2. The differentiated sorption of both dyes in order with the changing pH of the solution results in the electrostatic influence of adequate structural forms of the dyes with the surface of investigated carbons.

The adsorption process kinetics can be described by pseudo-second-order equation. The rate constants of the process increase with temperature rise. It should be mentioned that the intraparticle diffusion influence the whole process, but it isn't the limiting stage.

Adsorption data were substituted into theoretical equations: Langmuir, Freundlich, Langmuir–Freundlich, and Dubinin–Radushkevich. Applied mathematical models show that adsorption process description is Langmuir equation.

The following thermodynamic functions of adsorption process were calculated: free enthalpy $\Delta G°$, enthalpy $\Delta H°$, entropy $\Delta S°$, and isosteric heat of adsorption ΔH_x. The process has spontaneous ($\Delta G° < 0$) and endothermic ($\Delta H° > 0$) character. The $\Delta S°$ value is positive what indicates an increase in randomness at the solid/solution interface during dye adsorption. The isosteric heat of adsorption increases with the increase of surface coverage for ST-A (MB) and ST-A-CO_2 (MB).

It should be emphasized that mesoporous carbon modified by carbon dioxide (ST-A-CO_2) is a better adsorbent

Table 4
Parameters of the Langmuir, Langmuir–Freundlich, Freundlich, and Dubinin–Radushkevich adsorption isotherm models

Adsorbent (Adsorbate)	Isotherm	Parameters	Temperature		
			298 K	308 K	315 K
ST-A (MO)	Langmuir	$q_{m,exp}$ (mg g^{-1})	117	129	154
		q_m (mg g^{-1})	120	128	149
		K_L (dm^3 mg^{-1})	0.0638	0.0708	0.0788
		R^2	0.996	0.995	0.931
	Langmuir–Freundlich	q_m (mg g^{-1})	128	140	144
		K_{LF} (dm^3 mg^{-1})	0.0571	0.0606	0.0879
		M	0.7264	0.6657	5.084
		R^2	0.999	0.9995	0.986
	Freundlich	K_F (mg$^{1-1/n}$ (dm^3)$^{1/n}$ g^{-1})	31.14	34.99	51.216
		N	4.656	4.800	6.142
		R^2	0.956	0.964	0.897
	Dubinin–Radushkievich	q_m (mg g^{-1})	203	219	213
		β (mol^2 kJ^{-2})	1.845×10^{-9}	1.517×10^{-9}	1.851×10^{-9}
		E (kJ mol^{-1})	16.5	18.1	16.4
		R^2	0.966	0.790	0.972
ST-A-CO_2 (MO)	Langmuir	$q_{e,exp}$ (mg g^{-1})	323	326	330
		q_m (mg g^{-1})	315	323	327
		K_L (dm^3 mg^{-1})	0.0453	0.0506	0.0543
		R^2	0.984	0.901	0.946
	Langmuir–Freundlich	q_m (mg g^{-1})	326.22	321.29	327.6
		K_{LF} (dm^3 mg^{-1})	0.0524	0.0500	0.0534
		M	0.757	1.026	1.054
		R^2	0.885	0.901	0.946
	Freundlich	K_F (mg$^{1-1/n}$ (dm^3)$^{1/n}$ g^{-1})	147	153	154
		N	8.99	9.11	8.89
		R^2	0.858	0.860	0.877
	Dubinin–Radushkievich	q_m (mg g^{-1})	409	409	432
		β (mol^2 kJ^{-2})	1.266×10^{-9}	1.184×10^{-9}	1.127×10^{-9}
		E (kJ mol^{-1})	19.9	20.5	21.1
		R^2	0.870	0.870	0.901

ST-A (MB)	Langmuir	$q_{m,exp}$ (mg g^{-1})	135	139	187
		q_m (mg g^{-1})	135	142	188
		K_L (dm^3 mg^{-1})	0.0286	0.0320	0.0337
		R^2	0.989	0.976	0.959
	Langmuir–Freundlich	q_m (mg g^{-1})	143	162	211
		K_{LF} (dm^3 mg^{-1})	0.0239	0.0208	0.0142
		M	0.8251	0.6750	0.0577
		R^2	0.989	0.992	0.986
	Freundlich	K_F (mg$^{1-1/n}$ (dm^3)$^{1/n}$ g^{-1})	30.62	29.16	37.39
		N	4.40	4.08	3.90
		R^2	0.931	0.946	0.960
	Dubinin–Radushkievich	q_m (mg g^{-1})	237	259	358
		β (mol^2 kJ^{-2})	2.463 × 10^{-9}	2.385 × 10^{-9}	2.340 × 10^{-9}
		E (kJ mol^{-1})	14.2	14.5	14.6
		R^2	0.956	0.971	0.978
ST-A-CO_2 (MB)	Langmuir	$q_{m,exp}$ (mg g^{-1})	192	195	222
		q_m (mg g^{-1})	182	193	213
		K_L (dm^3 mg^{-1})	0.8910	0.9305	0.9640
		R^2	0.973	0.968	0.968
	Langmuir–Freundlich	q_m (mg g^{-1})	189	193	210
		K_{LF} (dm^3 mg^{-1})	0.7382	0.9306	1.0190
		M	0.835	1.029	1.162
		R^2	0.977	0.968	0.970
	Freundlich	K_F (mg$^{1-1/n}$ (dm^3)$^{1/n}$ g^{-1})	79.24	109.48	99.21
		N	6.08	9.37	6.68
		R^2	0.871	0.893	0.865
	Dubinin–Radushkievich	q_m (mg g^{-1})	304	265	333
		β (mol^2 kJ^{-2})	1.374 × 10^{-9}	0.870 × 10^{-9}	1.107 × 10^{-9}
		E (kJ mol^{-1})	19.1	24.0	21.2
		R^2	0.884	0.808	0.848

Table 5
Thermodynamic parameters for MO and MB adsorption on studied carbons

Adsorbent (adsorbate)	T (K)	$\Delta G°$ (kJ mol^{-1})	$\Delta H°$ (kJ mol^{-1})	$\Delta S°$ (J K^{-1} mol^{-1})
ST-A (MO)	298	–24.64	9.40	114.18
	308	–25.74		
	315	–26.60		
ST-A-CO_2 (MO)	298	–23.80	8.12	107.10
	308	–24.88		
	315	–25.62		
ST-A (MB)	298	–22.60	3.21	115.20
	308	–23.64		
	315	–24.30		
ST-A-CO_2 (MB)	298	–31.12	7.33	100.47
	308	–32.27		
	315	–33.08		

Table 6
Isosteric heat of OM an MB adsorption on tested carbon materials

Adsorbent (adsorbate)	q_e (mg g^{-1})	ΔH_x (kJ mol^{-1})	R^2
ST-A (MO)	70	13.92	0.928
	90	14.01	0.930
	110	7.90	0.680
ST-A-CO_2 (MO)	220	10.02	0.879
	240	10.03	0.880
	260	10.02	0.879
ST-A (MB)	81	35.97	0.935
	101	44.87	0.813
	120	58.57	0.792
ST-A-CO_2 (MB)	105	8.96	0.937
	130	36.68	0.985
	150	66.18	1

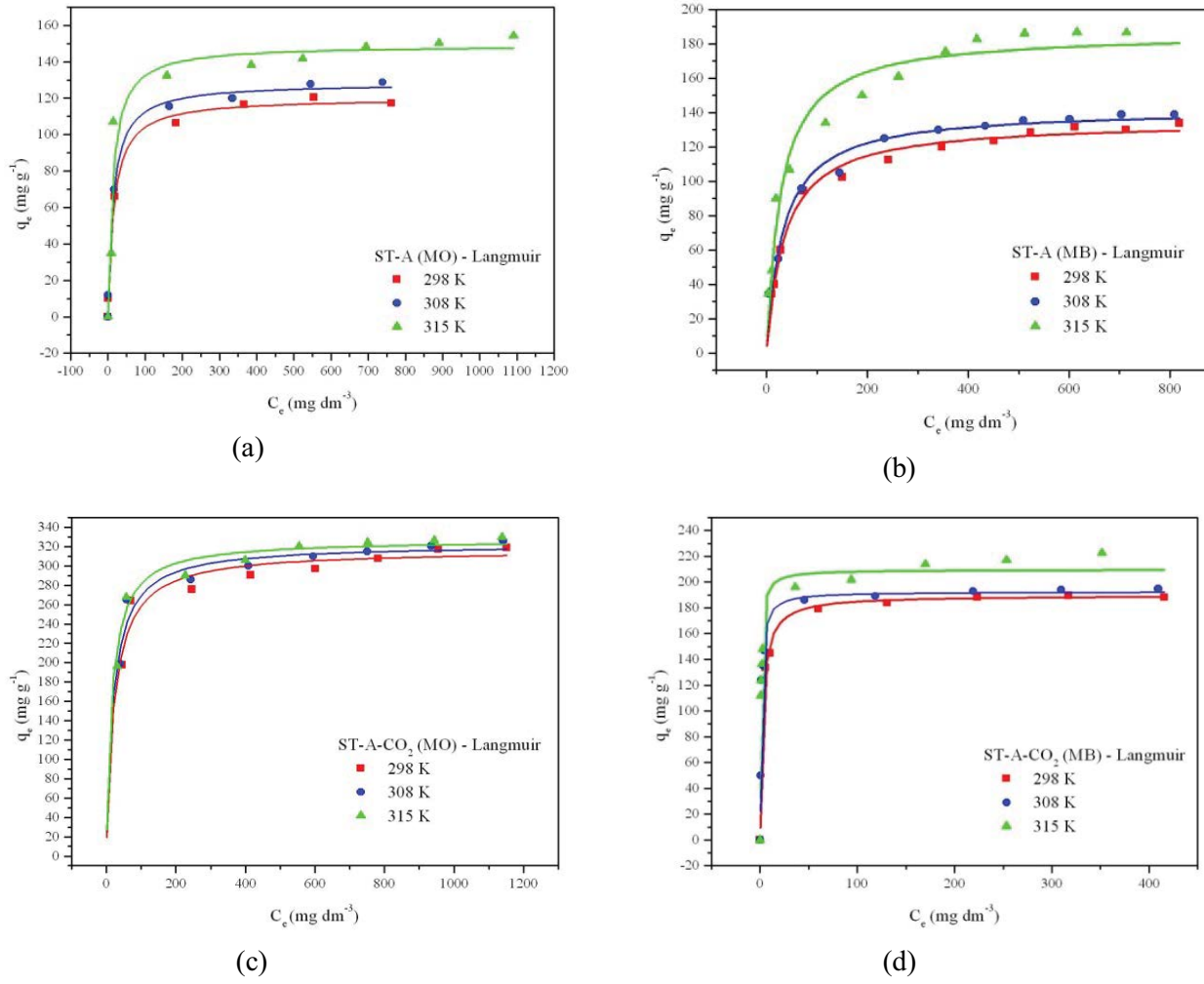

Fig. 12. Langmuir isotherms depending on the temperature for studied carbons (a and c) MO and (b and d) MB.

Table 7
Comparison between of studied in this work carbon materials with other adsorbents used in literature

Adsorbent	Adsorption capacity (MO) (mg g^{-1})	Adsorption capacity (MB) (mg g^{-1})	Reference
ST-A	117–154	135–187	This study
ST-A-CO_2	323–330	192–222	This study
C_{KIT-6}[a]	259	–	[2]
CCM[b]	102	–	[4]
FAC[c]	–	259–272	[12]
AC[d]	200	–	[16]
MAC[e]	293–318	355–364	[27]
CMK-3[f]	294	–	[48]
AC-SDVB[g]	556	556	[23]
OMC-PF[h]	115	104	[23]
AC-F400[i]	102	106	[23]
AC[j]	27.32	–	[25]
PAAC[k]	212.77–238.10	–	[26]
Nanoporous carbon[l]	18.8	–	[29]
NMC-3[m]	155.5	–	[53]
NMC-3-600[m]	170.1	–	[53]
NMC-3-810[m]	202.4	–	[53]
SS + TW biochar[n]	–	12.58–19.38	[30]
MAC[o]	–	162.87–192.31	[32]
SLS-C[p]	–	232.5	[44]
PAC-2[q]	–	345	[40]

[a]Ordered mesoporous carbons obtained using KIT-6 (hard template) and sucrose (carbon precursor), [b]cordierite monolith modified to carbonaceous material termed as carbon coated monolith, [c]biomass-based (pits) activated carbon obtained by $FeCl_3$ activation, [d]Jerusalem artichoke stalk based mesoporous activated carbon, [e]mesoporous carbon (hard template: SBA-15, carbon source: sucrose), [f]mesoporous carbon, [g]microporous carbon obtained from the polymer precursor – a sulphone-based styrene resin divinylbenzene, [h]mesoporous carbon material obtained from a phenol-formaldehyde resin by soft-templating method, [i]commercial carbon, [j]activated carbon prepared from dried pulp from the oak cups, [k]activated carbon derived from *Phragmites australis*, [l]hexagonal shaped nanoporous carbon synthesized using phenol and formaldehyde in the presence of triblock co-polymer P123 as soft template, [m]nitrogen-doped mesoporous carbon materials, [n]biochar prepared from co-pyrolysis of municipal sewage sludge and tea waste, [o]magnetic activated carbon prepared from eucalyptus sawdust (activation magnetization with $FeCl_3$), [p]activated carbon modified by anionic surfactants—sodium lauryl sulfate (SLS), [q]activated carbon produced by the steam activation of New Zealand bituminous coal on an industrial scale.

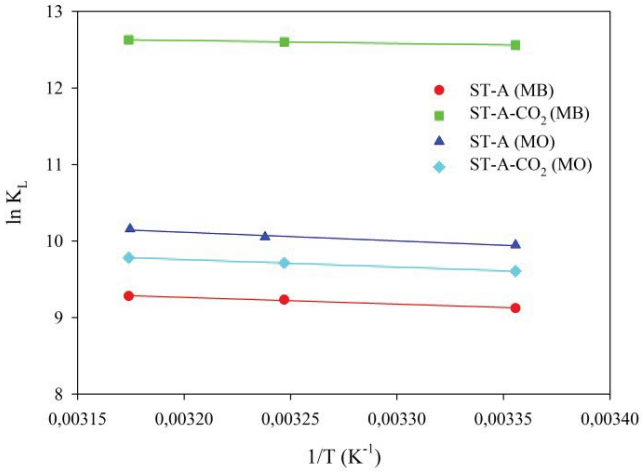

Fig. 13. Plot $\ln K_L = f(1/T)$ for all investigated adsorbents.

compared to unmodified mesoporous carbon ST-A. The better properties of the ST-A-CO_2 material are achieved by the slightly more developed porous structure, and thus the larger volume of micropores compared to carbon ST-A. This relationship is observed for both dyes tested. The maximum values of $q_{m,exp}$ at 315 K are for ST-A (MO): 154 mg g^{-1}, for ST-A-CO_2 (MO): 330 mg g^{-1}, ST-A (MB): 187 mg g^{-1}, and ST-A-CO_2 (MB): 222 mg g^{-1}.

Acknowledgments

This work was supported by Ministry of Science and Higher Education, Poland (research project SMGR. RN.20.263).

References

[1] I. Anastopoulos, A. Mittal, M. Usman, J. Mittal, G. Yu, A. Núñez-Delgado, M. Kornaros, A review on halloysite-based adsorbents

to remove pollutants in water and wastewater, J. Mol. Liq., 269 (2018) 855–868.
[2] J. Goscianska, M. Marciniak, R. Pietrzak, Mesoporous carbons modified with lanthanum(III) chloride for methyl orange adsorption, Chem. Eng. J., 247 (2014) 258–264.
[3] J. Choma, M. Czubaszek, M. Jaroniec, Adsorption of dyes from aqueous solutions on active carbons, Ochr. Sr., 37 (2015) 3–14 (in Polish).
[4] S. Hosseini, M.A. Khan, M.R. Malekbala, W. Cheah, T.S.Y. Choong, Carbon coated monolith, a mesoporous material for the removal of methyl orange from aqueous phase: adsorption and desorption studies, Chem. Eng. J., 171 (2011) 1124–1131.
[5] K. Lu, T. Wang, L. Zhai, W. Wu, S. Dong, S. Gao, L. Mao, Adsorption behavior and mechanism of Fe–Mn binary oxide nanoparticles: adsorption of methylene blue, J. Colloid Interface Sci., 539 (2019) 553–562.
[6] J. Mittal, Permissible synthetic food dyes in India, Resonance, 25 (2020) 567–577.
[7] A. Mittal, J. Mittal, Chapter 11: Hen Feather: A Remarkable Adsorbent for Dye Removal, S.K. Sharma, Ed., Green Chemistry for Dyes Removal from Wastewater, Scrivener Publishing LLC, USA, 2015, pp. 409–457.
[8] M.J.R.G.R. Pires, M.I.A. Ferra, A.M.M. Marques, Ionization of methyl orange in aqueous sodium chloride solutions, J. Chem. Thermodyn., 51 (2012) 93–99.
[9] I.S. Yahia, M.S. Abd El-Sadek, F. Yakuphanoglu, Methyl orange (C.I. acid orange 52) as a new organic semiconductor: conduction mechanism and dielectrical relaxation, Dyes Pigm., 93 (2012) 1434–1440.
[10] A. Mittal, V. Gajbe, J. Mittal, Removal and recovery of hazardous triphenylmethane dye, Methyl Violet through adsorption over granulated waste materials, J. Hazard. Mater., 150 (2008) 364–375.
[11] Z. Ezzeddine, I. Batonneau-Gener, Y. Pouilloux, H. Hamad, Removal of methylene blue by mesoporous CMK-3: kinetics, isotherms and thermodynamics, J. Mol. Liq., 223 (2016) 763–770.
[12] S.K. Theydan, M.J. Ahmed, Adsorption of methylene blue onto biomass-based activated carbon by $FeCl_3$ activation: equilibrium, kinetics, and thermodynamic studies, J. Anal. Appl. Pyrolysis, 97 (2012) 116–122.
[13] F.M. Maingi, H.M. Mbuvi, M.M. Ng'ang'a, H. Mwangi, Adsorption kinetics and isotherms of methylene blue by geopolymers derived from common clay and rice husk ash, Phys. Chem., 7 (2017) 87–97.
[14] H. Daraei, A. Mittal, Investigation of adsorption performance of activated carbon prepared from waste tire for the removal of methylene blue dye from wastewater, Desal. Water Treat., 90 (2017) 294–298.
[15] S. Soni, P.K. Bajpai, J. Mittal, C. Arora, Utilisation of cobalt doped Iron based MOF for enhanced removal and recovery of methylene blue dye from waste water, J. Mol. Liq., 314 (2020) 113642–113653.
[16] A. Bellifa, M. Makhlouf, Z.H. Boumila, Comparative study of the adsorption of methyl orange by bentonite and activated carbon, Acta Phys. Pol. A, 132 (2017) 466–468.
[17] V.K. Gupta, S. Agarwal, R. Ahmad, A. Mirza, J. Mittal, Sequestration of toxic congo red dye from aqueous solution using ecofriendly guar gum/activated carbon nanocomposite, Int. J. Biol. Macromol., 158 (2020) 1310–1318.
[18] F. Liu, Z. Guo, H. Ling, Z. Huang, D. Tang, Effect of pore structure on the adsorption of aqueous dyes to ordered mesoporous carbons, Microporous Mesoporous Mater., 227 (2016) 104–111.
[19] A. Chen, Y. Li, Y. Yu, Y. Li, K. Xia, Y. Wang, S. Li, Synthesis of mesoporous carbon nanospheres for highly efficient adsorption of bulky dye molecules, J. Mater. Sci., 51 (2016) 7016–7028.
[20] A. Mittal, V. Thakur, V. Gajbe, Evaluation of adsorption characteristics of an anionic azo dye Brilliant Yellow onto hen feathers in aqueous solutions, Environ. Sci. Pollut. Res., 19 (2012) 2438–2447.
[21] J. Mittal, V. Thakur, A. Mittal, Batch removal of hazardous azo dye Bismark Brown R using waste material hen feather, Ecol. Eng., 60 (2013) 249–253.
[22] A. Mittal, R. Jain, J. Mittal, M. Shrivastava, Adsorptive removal of hazardous dye quinoline yellow from waste water using coconut-husk as potential adsorbent, Fresenius Environ. Bull., 19 (2010) 1–9.
[23] M. Czubaszek, J. Choma, Adsorption of dyes from aqueous solutions on nanoporous carbon materials obtained from polymeric precursors, Ochr. Sr., 39 (2017) 3–10 (in Polish).
[24] M. Czubaszek, J. Choma, Kinetic studies of selected dye adsorption from aqueous solutions on nanoporous carbons obtained from polymeric precursors, Ochr. Sr., 38 (2016) 3–12 (in Polish).
[25] E. Ghasemian, Z. Palizban, Comparisons of azo dye adsorption onto activated carbon and silicon carbide nanoparticles loaded on activated carbon, Int. J. Environ. Sci. Technol., 13 (2016) 501–512.
[26] S. Chen, J. Zhang, C. Zhang, Q. Yue, Y. Li, C. Li, Equilibrium and kinetic studies of methyl orange and methyl violet adsorption on activated carbon derived from *Phragmites australis*, Desalination, 252 (2010) 149–156.
[27] L. Yu, Y. Luo, The adsorption mechanism of anionic and cationic dyes by Jerusalem artichoke stalk-based mesoporous activated carbon, J. Environ. Chem. Eng., 2 (2014) 220–229.
[28] D. Zhao, W. Zhang, C. Chen, X. Wang, Adsorption of methyl orange dye onto multiwalled carbon nanotubes, Procedia Environ. Sci., 18 (2013) 890–895.
[29] S. Kundu, I.H. Chowdhury, M.K. Naskar, Synthesis of hexagonal shaped nanoporous carbon for efficient adsorption of methyl orange dye, J. Mol. Liq., 234 (2017) 417–423.
[30] S. Fan, J. Tang, Y. Wang, H. Li, H. Zhang, J. Tang, Z. Wang, X. Li, Biochar prepared from co-pyrolysis of municipal sewage sludge and tea waste for the adsorption of methylene blue from aqueous solutions: kinetics, isotherm, thermodynamic and mechanism, J. Mol. Liq., 220 (2016) 432–441.
[31] A.H. Jawad, R. Razuan, J.N. Appaturi, L.D. Wilson, Adsorption and mechanism study for methylene blue dye removal with carbonized watermelon (*Citrullus lanatus*) rind prepared via one-step liquid phase H_2SO_4 activation, Surf. Interfaces, 16 (2019) 76–84.
[32] C. Chen, S. Mi, D. Lao, P. Shi, Z. Tong, Z. Li, H. Hu, Single-step synthesis of eucalyptus sawdust magnetic activated carbon and its adsorption behavior for methylene blue, RSC Adv., 9 (2019) 22248–22262.
[33] I.A. Tan, A.L. Ahmad, B.H. Hameed, Adsorption of basic dye on high-surface-area activated carbon prepared from coconut husk: equilibrium, kinetic and thermodynamic studies, J. Hazard. Mater., 154 (2008) 337–346.
[34] M.U. Dural, L. Cavas, S.K. Papageorgiou, F.K. Katsaros, Methylene blue adsorption on activated carbon prepared from *Posidonia oceanica* (L.) dead leaves: kinetic and equilibrium studies, Chem. Eng. J., 168 (2011) 77–85.
[35] D. Kavitha, C. Namasivayam, Experimental and kinetics studies on methylene blue adsorption by coir path carbon, Bioresour. Technol., 98 (2007) 14–21.
[36] M. Zubair, N.D. Mu'azu, N. Jarrah, N.I. Blaisi, H.A. Aziz, M.A. Al-Harthi, Adsorption behavior and mechanism of methylene blue, crystal violet, Eriochrome Black T, and Methyl Orange dyes onto biochar-derived date palm fronds waste produced at different pyrolysis conditions, Water Air Soil Pollut., 231 (2020) 240–259.
[37] N. Kannan, M.M. Sundaram, Kinetics and mechanism of removal of methylene blue by adsorption on various carbons - a comparative study, Dyes Pigm., 51 (2001) 25–40.
[38] Z. Jia, Z. Li, S. Li, Y. Li, R. Zhu, Adsorption performance and mechanism of methylene blue on chemically activated carbon spheres derived from hydrothermally-prepared poly(vinyl alcohol) microspheres, J. Mol. Liq., 220 (2016) 56–62.
[39] Y. Kuang, X. Zhang, S. Zhou, Adsorption of methylene blue in water onto activated carbon by surfactant modification, Water, 12 (2020) 587–605.
[40] E.N.E. Qada, S.J. Allen, G.M. Walker, Adsorption of Methylene Blue onto activated carbon produced from steam activated bituminous coal: a study of equilibrium adsorption isotherm, Chem. Eng. J., 124 (2006) 103–110.

[41] F.C. Wu, R.L. Tseng, C.C. Hu, Comparisons of pore properties and adsorption performance of KOH-activated and steam-activated carbons, Microporous Mesoporous Mater., 80 (2005) 95–106.
[42] P. Hadi, K.Y. Yeung, J. Barford, K.J. An, G. McKay, Significance of "effective" surface area of activated carbons on elucidating the adsorption mechanism of large dye molecules, J. Environ. Chem. Eng., 3 (2015) 1029–1037.
[43] P. Wang, M. Cao, C. Wang, Y. Ao, J. Hou, J. Qian, Kinetics and thermodynamics of adsorption of methylene blue by a magnetic graphene-carbon nanotube composite, Appl. Surf. Sci., 290 (2014) 116–124.
[44] L. Liu, S. Fan, Y. Li, Removal behavior of methylene blue from aqueous solution by tea waste: kinetics, isotherms and mechanism, Int. J. Environ. Res. Public Health, 15 (2018) 1321–1336.
[45] V.-P. Dinh, T.-D.-T. Huynh, H.M. Le, V.-D. Nguyen, V.-A. Dao, N.Q. Hung, L.A. Tuyen, S. Lee, J. Yi, T.D. Nguyen, L.V. Tan, Insight into the adsorption mechanisms of methylene blue and chromium(III) from aqueous solution onto pomelo fruit peel, RSC Adv., 9 (2019) 25847–25860.
[46] R. Han, J. Zhang, P. Han, Y. Wang, Z. Zhao, M. Tang, Study of equilibrium, kinetic and thermodynamic parameters about methylene blue adsorption onto natural zeolite, Chem. Eng. J., 145 (2009) 496–504.
[47] C. Arora, S. Soni, S. Sahu, J. Mittal, P. Kumar, P.K. Bajpai, Iron based metal organic framework for efficient removal of methylene blue dye from industrial waste, J. Mol. Liq., 284 (2019) 343–352.
[48] N. Mohammadi, H. Khani, V.K. Gupta, E. Amereh, S. Agarwal, Adsorption process of methyl orange dye onto mesoporous carbon material-kinetic and thermodynamic studies, J. Colloid Interface Sci., 362 (2011) 457–462.
[49] A. Derylo-Marczewska, A.W. Marczewski, S. Winter, D. Sternik, Studies of adsorption equilibria and kinetics in the system: aqueous solution of dye-mesoporous carbons, Appl. Surf. Sci., 256 (2010) 5164–5170.
[50] S. Asuha, X.G. Zhou, S. Zhao, Adsorption of methyl orange and Cr(VI) on mesoporous TiO_2 prepared by hydrothermal method, J. Hazard. Mater., 181 (2010) 204–210.
[51] N. Liu, L. Yin, L. Zhang, C. Wang, N. Lun, Y. Qi, C. Wang, Ferromagnetic Ni decorated ordered mesoporous carbons as magnetically separable adsorbents for methyl orange, Mater. Chem. Phys., 131 (2011) 52–59.
[52] T.M. Albayati, G.M. Alwan, O.S. Mahdy, High performance methyl orange capture on magnetic nanoporous MCM-41 prepared by incipient wetness impregnation method, Korean J. Chem. Eng., 34 (2017) 259–265.
[53] H. Li, N. An, G. Liu, J. Li, N. Liu, M. Jia, W. Zhang, X. Yuan, Adsorption behaviors of methyl orange dye on nitrogen-doped mesoporous carbon materials, J. Colloid Interface Sci., 466 (2016) 343–351.
[54] W. Cheah, S. Hosseini, M.A. Khan, T.G. Ghuah, T.S.Y. Choong, Acid modified carbon coated monolith for methyl orange adsorption, Chem. Eng. J., 215–216 (2013) 747–754.
[55] X. Li, H. Yuan, X. Quan, S. Chen, S. You, Effective adsorption of sulfamethoxazole, bisphenol A and methyl orange on nanoporous carbon derived from metal-organic frameworks, J. Environ. Sci., 63 (2018) 250–259.
[56] T.A. Saleh, A.A. Al-Saadi, V.K. Gupta, Carbonaceous adsorbent prepared from waste tires: experimental and computational evaluations of organic dye methyl orange, J. Mol. Liq., 191 (2014) 85–91.
[57] K. Jedynak, M. Repelewicz, K. Kurdziel, D. Wideł, Removal of orange II from aqueous solutions using micro-mesoporous carbon materials: kinetic and equilibrium studies, Desal. Water Treat., 190 (2020) 294–311.
[58] X. Wang, C.D. Liang, S. Dai, Facile synthesis of ordered mesoporous carbons with high thermal stability by self-assembly of resorcinol–formaldehyde and block copolymers under highly acidic conditions, Langmuir, 24 (2008) 7500–7505.
[59] J. Choma, A. Kalinowska, K. Jedynak, M. Jaroniec, Reproducibility of the synthesis and adsorption properties of ordered mesoporous carbons obtained by the soft-templating method, Ochr. Sr., 34 (2012) 1–8 (in Polish).
[60] N.P. Wickramaratne, M. Jaroniec, Activated carbon spheres for CO_2 adsorption, ACS Appl. Mater. Interfaces, 5 (2013) 1849–1855.
[61] Y. Zhou, L. Sun, H. Wang, W. Liang, J. Yang, L. Wang, S. Shuang, Investigation on the uptake and release ability of b-cyclodextrin functionalized Fe_3O_4 magnetic nanoparticles by methylene blue, Mater. Chem. Phys., 170 (2016) 83–89.
[62] K. Kurdziel, M. Raczyńska-Żak, L. Dąbek, Equilibrium and kinetic studies on the process of removing chromium(VI) from solutions using HDTMA-modified halloysite, Desal. Water Treat., 137 (2019) 88–100.
[63] F. Marrakchi, M.J. Ahmed, W.A. Khanday, M. Asif, B.H. Hameed, Mesoporous-activated carbon prepared from chitosan flakes via single-step sodium hydroxide activation for the adsorption of methylene blue, Int. J. Biol. Macromol., 98 (2017) 233–239.
[64] C.K. Lim, H.H. Bay, C.H. Noeh, A. Aris, Z.A. Majid, Z. Ibrahim, Application of zeolite-activated carbon macrocomposite for the adsorption of Acid Orange 7: isotherm, kinetic and thermodynamic studies, Environ. Sci. Pollut. Res., 20 (2013) 7243–7255.
[65] Y.S. Al-Degs, M.I. El-Barghouthi, A.H. El-Sheikh, G.M. Walker, Effect of solution pH, ionic strength, and temperature on adsorption behavior of reactive dyes on activated carbon, Dyes Pigm., 77 (2008) 16–23.
[66] S. Lagergren, About the theory of so-called adsorption of soluble substances, Kungl. Sven. Veten. Akad. Handl, 24 (1898) 1–39.
[67] Y.S. Ho, G. McKay, Pseudo-second-order model for sorption processes, Process Biochem., 34 (1999) 451–465.
[68] W.J. Weber, J.C. Morris, Kinetics of adsorption on carbon solution, J. Sanitary Eng. Div. Am. Soc. Civ. Eng., 89 (1963) 31–59.
[69] X. Li, G. Wang, W. Li, P. Wang, C. Su, Adsorption of acid and basic dyes by sludge-based activated carbon: isotherm and kinetic studies, J. Cent. South Univ., 22 (2015) 103–113.
[70] I. Langmuir, The constitution and fundamental properties of solids and liquids. Part I. Solids, J. Am. Chem. Soc., 38 (1916) 2221–2295.
[71] H.M.F. Freundlich, Over the adsorption in solution, J. Phys. Chem., 57 (1906) 385–470.
[72] M.M. Dubinin, L.V. Radushkevich, The equation of the characteristic curve of activated charcoal, Proc. Acad. Sci. USSR, 55 (1947) 331–337.
[73] M.M. Dubinin, The potential theory of adsorption of gasses and vapors for adsorbents with energetically nonuniform surfaces, Chem. Rev., 60 (1960) 235–266.
[74] S. Chowdhury, R. Mishra, P. Saha, P. Kushwaha, Adsorption thermodynamics, kinetics and isosteric heat of adsorption of malachite green onto chemically modified rice husk, Desalination, 265 (2011) 159–168.